Structural behavior of ^{157,158,159}Dy in the $I = 30$–$50\hbar$ spin regime

A. Pipidis,[1] M. A. Riley,[1] J. Simpson,[2] R. V. F. Janssens,[3] F. G. Kondev,[3,4] D. E. Appelbe,[2] A. P. Bagshaw,[5] M. A. Bentley,[6] T. B. Brown,[7] M. P. Carpenter,[3] D. M. Cullen,[5] D. B. Campbell,[1] P. J. Dagnall,[5] P. Fallon,[8] S. M. Fischer,[3,*] G. B. Hagemann,[9] D. J. Hartley,[10] K. Lagergren,[1] R. W. Laird,[1] T. Lauritsen,[3] J. C. Lisle,[5] D. Nisius,[3] S. L. Shepherd,[11] A. G. Smith,[5] S. Törmänen,[9] and I. Ragnarsson[12]

[1]*Department of Physics, Florida State University, Tallahassee, Florida 32306, USA*
[2]*CCLRC Daresbury Laboratory, Daresbury, Warrington WA4 4AD, United Kingdom*
[3]*Physics Division, Argonne National Laboratory, Argonne, Illinois 60439, USA*
[4]*Nuclear Engineering, Argonne National Laboratory, Argonne, Illinois 60439, USA*
[5]*Schuster Laboratory, University of Manchester, Manchester M13 9PL, United Kingdom*
[6]*Department of Physics, Keele University, Staffordshire ST5 5BG, United Kingdom*
[7]*Savannah River Technology Center, Westinghouse Savannah River Company, Aiken, South Carolina 29802, USA*
[8]*Nuclear Science Division, Lawrence Berkeley National Laboratory, Berkeley, California 94720, USA*
[9]*The Niels Bohr Institute, University of Copenhagen, Blegdamsvej 17, 2100 Copenhagen, Denmark*
[10]*Department of Physics, United States Naval Academy, Annapolis, Maryland 21402, USA*
[11]*Oliver Lodge Laboratory, University of Liverpool, Liverpool L69 7ZE, United Kingdom*
[12]*Department of Mathematical Physics, Lund Institute of Technology, Box 118, S-221 00, Lund, Sweden*

(Received 14 February 2005; published 13 December 2005)

Significant extensions to the high-spin excitation spectrum of the $N = 91$, 92, 93 isotopes ^{157,158,159}Dy have been achieved using the high-efficiency γ-ray spectrometers Euroball and Gammasphere. These nuclei were populated via weak $3n$ or αxn exit channels in fusion evaporation reactions. In ^{157}Dy, the yrast band has been extended to $I^{\pi} = \frac{101}{2}^{+}$ (tentatively to $\frac{105}{2}^{+}$) with four sideband structures (two of which are new) observed in the 35–50$\hbar$ spin range. In ^{158}Dy, three bands have been extended to $42^{+}(44^{+})$, 40^{-}, and $41^{-}(43^{-})$, whereas in ^{159}Dy the yrast band is observed to $\frac{81}{2}^{+}$ ($\frac{85}{2}^{+}$). The high-spin behavior and band crossing systematics of the Dy isotopes and of the neighboring $N = 91$, 92, and 93 isotones are discussed in terms of rotational alignments and shape transitions. Cranked Nilsson-Strutinsky calculations without pairing have been performed for detailed comparisons with the very high-spin states observed in ^{157}Dy.

DOI: 10.1103/PhysRevC.72.064307 PACS number(s): 27.70.+q, 21.10.Re, 23.20.Lv

I. INTRODUCTION

The observation of states of increasingly high angular momentum in nuclei, and the resulting rich variety of phenomena that occur, has been made possible by the availability of sophisticated detector systems. The current state-of-the-art, high-resolution γ-ray detector arrays, exemplified by Euroball [1] and Gammasphere [2,3], continue to chart new regions of angular momentum and excitation energy in nuclei throughout the periodic table. It is in the light $A \sim 160$ Dy and Er nuclei that the highest spin states in normal deformed nuclei have been systematically observed ($I \sim 60\hbar$ and $E_{\rm excit} \sim$ 30 MeV) [4–11]. A specific pattern of particle alignments is expected to emerge in these nuclei that allows the extraction of information on nuclear pairing correlations, as well as on the configuration dependence of nuclear deformation. At high spins ($I \geqslant 30\hbar$), dramatic changes in shape have been observed in $N = 88$–90 Dy and Er nuclei [11–23], and evidence for so-called "unpaired" band crossings has been obtained in $N \geqslant 91$ Er nuclei [4–8], providing detailed information on the single-particle spectrum of states involved. In the present work, significant extensions into the $I = 30$–$50\hbar$ spin regime have been made for the level schemes of $N = 91$, 92, and 93 Dy isotopes (^{157,158,159}Dy). The high-spin behavior of these Dy nuclei and their neighboring isotones is discussed in terms of rotational alignments, deformation differences, and shape transitions.

II. EXPERIMENTAL DETAILS

The nucleus ^{157}Dy was populated at high spin using the ^{124}Sn(^{36}S,$3n$)^{157}Dy reaction. The 165-MeV beam was provided by the 88-inch Cyclotron at Lawrence Berkeley National Laboratory, USA. The target consisted of two stacked 400-μg cm^{-2}-thick foils of isotopic ^{124}Sn. The deexcitation γ rays were detected by the Gammasphere array, which comprised 93 large-volume Compton-suppressed Ge detectors. The event trigger required five or more Compton-suppressed Ge detectors to fire in prompt coincidence. A total of 1.3×10^{9} events were collected. This experiment was primarily aimed at the spectroscopy of ^{156}Dy using the dominant $4n$ reaction channel [11]. The cross section for the $3n$ channel populating ^{157}Dy was only $\leqslant$3% of the total reaction cross section.

The nuclei ^{158,159}Dy were populated at high spin using the reaction ^{130}Te(^{36}S,αxn) at a beam energy of 170 MeV. The beam was provided by the tandem accelerator at the Laboratori Nazionali di Legnaro, Italy. The target consisted of two stacked foils of ^{130}Te, each of thickness 0.5 mg cm^{-2} with a 0.5 mg cm^{-2} Au backing. The primary aim of this experiment was

*Present address: Department of Physics, DePaul University, Chicago, Illinois 60614-3504, USA.

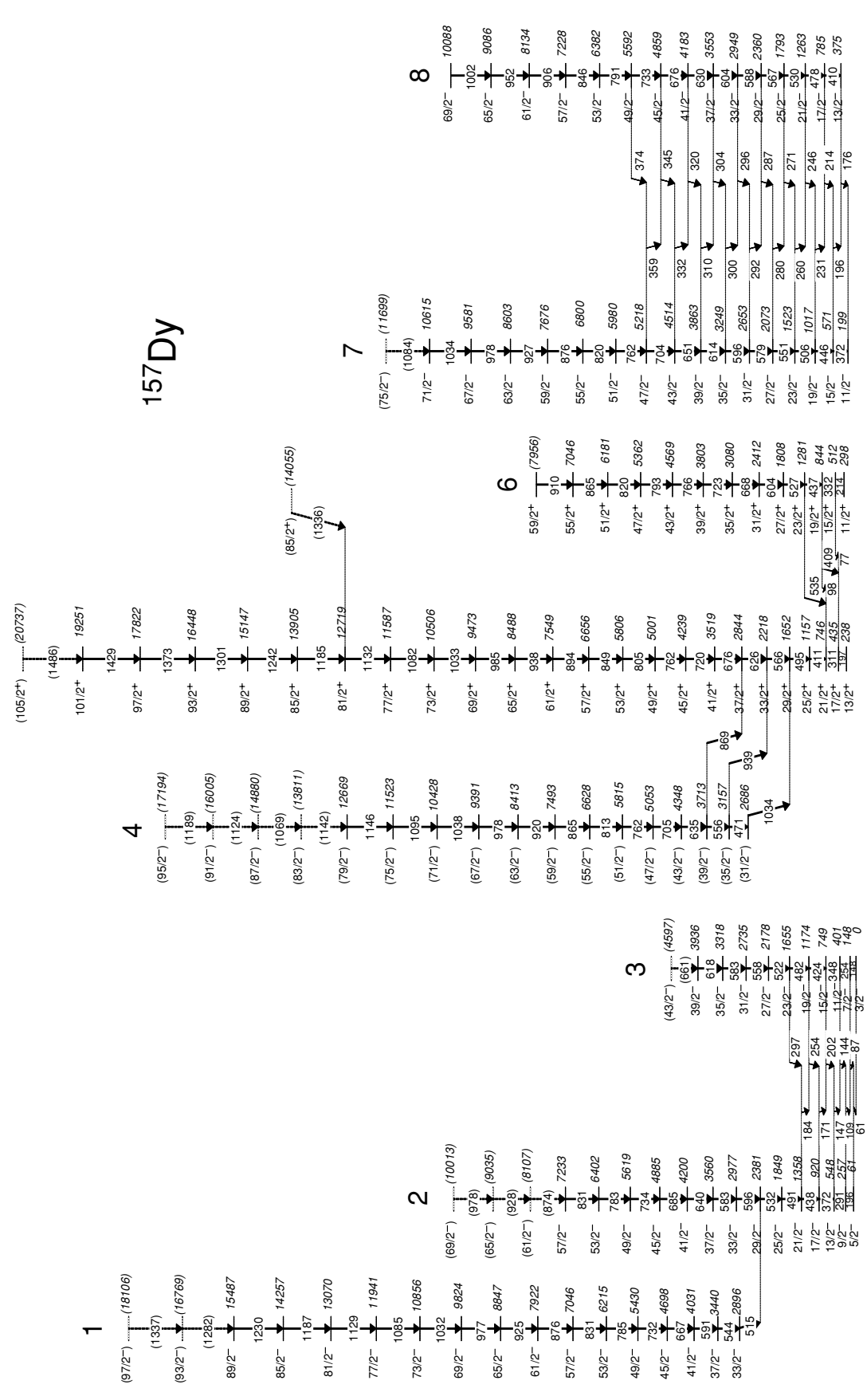

FIG. 1. Level scheme for ^{157}Dy deduced in this work. Energies are given in kiloelectronvolts; tentative transitions and levels are indicated by dotted lines; and tentative spin, parity, and level energies are given within parentheses.

to study high-spin states in the nuclei ^{161,162}Er [8] populated by the dominant xn reaction channels. The cross sections for the $\alpha 3n$ and $\alpha 4n$ exit channels corresponding to ^{158,159}Dy were only about 1 and 2%, respectively, of the total reaction cross section. The deexcitation γ rays were detected in the high-efficiency array Euroball III. The array consisted of 14 seven-element Cluster detectors [24], 26 four-element Clover detectors [25], and 30 single-crystal Ge detectors [26]. All the Ge detectors were Compton suppressed. The data were unfolded into 2×10^{10} γ^3 coincidence events.

A third experiment, primarily aimed at the investigation of high-spin states in ^{159,160}Er, was carried out using the reaction ^{130}Te(^{34}S, xn) at a bombarding energy of 170 MeV. The same targets as for the Euroball III measurements were used. The beam was obtained from the Vivitron accelerator at the Institut de Recherches Subatomiques, Strasbourg, France. The γ rays were detected with the Euroball IV spectrometer, which included the same complement of detectors as Euroball III, as well as a BGO inner ball for γ-ray multiplicity and sum-energy calorimetry measurements. Approximately 2×10^9 events were recorded. The inner ball was used to select very high-spin states by requiring a high-multiplicity condition on the BGO ball data. Information on ^{157}Dy was obtained via the weak ($\approx$1%) $\alpha 3n$ particle evaporation channel.

The unfolded γ^3 and γ^4 events in the above-mentioned experiments were analyzed using the RADWARE software analysis packages LEVIT8R and 4DG8R [27].

III. EXPERIMENTAL RESULTS

The level scheme for ^{157}Dy deduced in the present work is shown in Fig. 1. The majority of the new information was obtained from the Gammasphere data, although useful information for the very top of the yrast band was extracted from the Euroball IV data set. Spin-parity assignments at low spin are adopted from Refs. [28–30]. All the sequences continue with rotational-like behavior to higher spin, and therefore the new in-band transitions reported here are assumed to be of stretched electric quadrupole ($E2$) character.

The yrast ([651]3/2) band in ^{157}Dy (band 5) was previously observed to $\frac{81}{2}^+$ in Ref. [29]. In a recent study by Hayakawa *et al.* [30] several sidebands were established. The two [521]3/2 sequences (bands 2 and 3) were observed up to $\frac{37}{2}^-$ and $\frac{39}{2}^-$ (tentatively $\frac{41}{2}^-$ and $\frac{43}{2}^-$), the unfavored $i_{13/2}$ [651]3/2 signature (band 6) to $\frac{47}{2}^+$ and the two signatures of the [505]11/2 orbital (bands 7 and 8) to $\frac{43}{2}^-$ and $\frac{45}{2}^-$. The spectra obtained from a sum of triple coincidences within these bands using four-fold histograms from the Euroball IV and Gammasphere data are displayed in Figs. 2–4. The yrast sequence [band 5 (Fig. 2)] has been extended by six transitions to a spin value of $\frac{101}{2}^+$ (tentatively $\frac{105}{2}^+$). The unfavored $i_{13/2}$ [651]3/2 signature (band 6) has been delineated further by three transitions to a spin value of $\frac{59}{2}^+$. A new sequence (band 1) was observed which feeds into the favored signature of the [521]3/2 band (band 2) at $\frac{29}{2}^-$. Band 1 is traced to a tentative $\frac{97}{2}^-$ state, as shown in [Fig. 3(b)]. The [505]11/2 bands

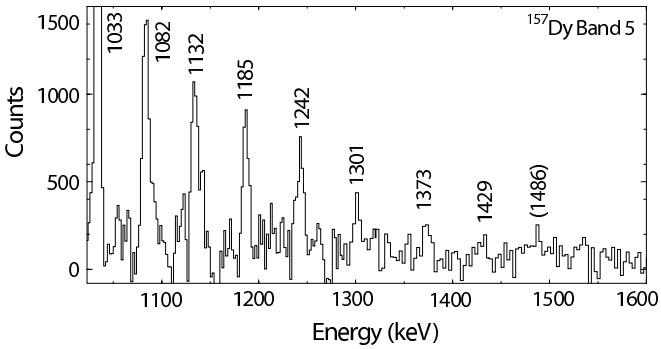

FIG. 2. High-energy part of a triple gated, summed coincidence spectrum for the yrast band (band 5) in ^{157}Dy obtained from the Euroball IV experiment.

(bands 7 and 8) are extended to spin values of ($\frac{75}{2}^-$) and $\frac{69}{2}^-$, respectively (Fig. 4(b)). In addition, another new sequence (band 4) was observed, see Fig. 4(a). The latter sequence has been assigned tentative spin values from $\frac{31}{2}^-$ to $\frac{95}{2}^-$.

Level schemes for ^{158,159}Dy as deduced from the present work are presented in Fig. 5. In ^{158}Dy, bands 1, 2, and 3 have been extended from $28^+, 25^-$, and 28^- [31] to 42^+ (44^+), 40^-, and 41^- (43^-), respectively. The yrast sequence in ^{159}Dy, band 1 (i.e., the favored $i_{13/2}$[642]5/2 $\alpha = +\frac{1}{2}$ signature), has been delineated from $\frac{61}{2}^+$ [32] to $\frac{81}{2}^+$ ($\frac{85}{2}^+$). Spin-parity assignments are taken from Refs. [31–35]. All sequences continue with rotational-like behavior to higher

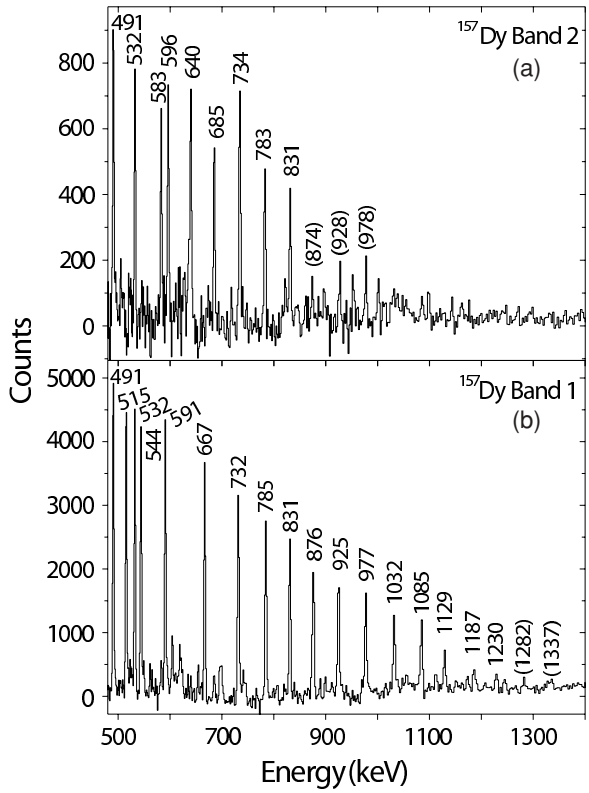

FIG. 3. Triple-gated, summed coincidence spectra for (a) band 2 and (b) band 1 in ^{157}Dy derived from the Gammasphere experiment.

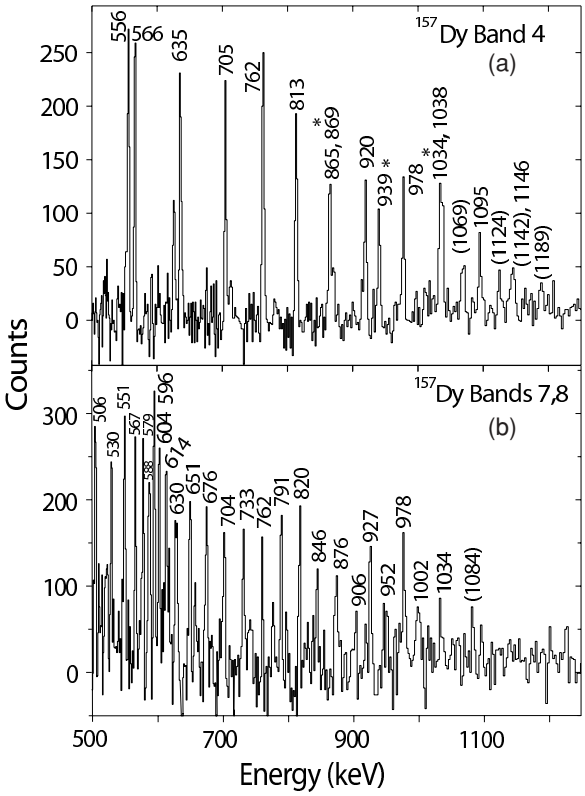

FIG. 4. Triple-gated, summed coincidence spectra for (a) band 4 and (b) bands 7 and 8 in ^{157}Dy obtained from the Gammasphere experiment.

spins and, therefore, the new in-band transitions observed in this work are again assumed to be of stretched $E2$ character. Figures 6(a), (b), and (c) provide examples of double-gated coincidence spectra obtained from these data for band 1 [which has been assigned parity and signature $(\pi,\alpha) = (+, 0)$], band 2 $(-,0)$, and band 3 $(-,1)$ sequences in ^{158}Dy, respectively. A double-gated spectrum for the yrast sequence (band 1) in ^{159}Dy is shown in Fig. 6(d).

IV. DISCUSSION

Experimentally deduced aligned angular momenta [36] (or alignments) versus rotational frequency for the bands in ^{157}Dy and ^{158}Dy are plotted in Figs. 7 and 8, respectively. The quasiparticle labeling scheme for the bands of given (π, α) uses the convention of Ref. [37]. A representative cranked-shell-model (CSM) calculation for ^{158}Dy (which is also useful for ^{157,159}Dy) can be found in Ref. [36]. The CSM has become a standard model with which to understand the excitation spectrum of rotating rare-earth nuclei. These calculations predict band crossings in this region of nuclei to be because of the alignment of the first (AB), second (BC), or third (AD) pairs of $i_{13/2}$ quasineutrons in the rotational frequency range $\hbar\omega = 0.25$–0.40 MeV. Above $\hbar\omega = 0.40$ MeV a similar set of alignments involving the first (A_pB_p), second (B_pC_p), and third (A_pD_p) pairs of $h_{11/2}$ quasiprotons is expected. The systematics of the experimental band-crossing frequencies, gains in aligned angular momenta, and interaction strengths can be compared with the CSM predictions.

In Figs. 7 and 8, the subtracted reference was based on the Harris parametrization [36] with the values $\Im_0 = 32.1\hbar^{-1}$ MeV^2 and $\Im_1 = 34.0\hbar^{-3}$ MeV^4. This reference gives a constant alignment for the $(-, +\frac{1}{2})$ three-quasiparticle configuration (B_pAB) in the odd-proton neighboring nucleus ^{157}Ho [38], which is also displayed in Figs. 7 and 8 as a dotted reference trajectory. This set of reference parameters is convenient when comparing the high-spin alignment properties in the neighboring nuclei, because the second and third neutron $i_{13/2}$ crossings BC and AD, as well as the first and second $h_{11/2}$ proton alignments A_pB_p and B_pC_p, are blocked for this configuration. The approximate rotational frequencies of various band crossings are indicated in Figs. 7 and 8 and are discussed in more detail below in the context of the systematic behavior of neighboring nuclei. Note that the major new high-spin sequences in ^{157}Dy (bands 1 and 4) track each other very closely in their alignment behavior and appear to form a natural signature pair. This is consistent with our tentative spin and parity assignment for band 4 (see also Fig. 11).

The alignments of the yrast $(+, +\frac{1}{2})$ bands in the odd-A, $N = 89$, 91, and 93 Dy nuclei are given in Fig. 9(a). All these bands experience a gradual but large gain in alignment from $\hbar\omega \approx 0.25$ to 0.6 MeV. This smooth gain is interpreted as originating from the alignment of the second pair of $i_{13/2}$ neutrons (BC) near $\hbar\omega = 0.35$ MeV, closely followed by the first proton $h_{11/2}$ (A_pB_p) crossing near $\hbar\omega = 0.45$ MeV. The gain of approximately $11\hbar$ is consistent with this interpretation since the BC and A_pB_p crossings are known to produce alignments of around $5\hbar$ and $6\hbar$, respectively [39]. Thus, by using the B_pAB configuration in ^{157}Ho as a reference (combined with comparisons with neighboring nuclei), an explanation of the "anomalous" BC alignment in ^{159}Dy discussed by Liang *et al.* [34] can be found. It is a consequence of a very gradual alignment caused by a strong interaction strength for the BC (and A_pB_p) crossing(s).

The structure of these odd-A Dy yrast bands can be considered to evolve from a single-quasineutron configuration (A) at low spin, to a five-quasiparticle configuration $(ABCA_pB_p)$ at high rotational frequencies. The negative-parity sidebands (bands 2 and 3) in ^{158}Dy (see Fig. 8) display the same gradual neutron (BC) and proton (A_pB_p) alignments at high spin. In the yrast $(+,0)$ band (band 1) of ^{158}Dy, the first $i_{13/2}$ neutron (AB) crossing occurs at $\hbar\omega = 0.3$ MeV. This crossing is also present in the ^{157}Ho reference band, which at low rotational frequencies is the $h_{11/2}$ one-quasiproton configuration B_p. In ^{157}Dy, (see Fig. 7), all the structures except bands 5 and 6, which start out with very small alignment ($<3\hbar$) at low frequencies, undergo an even larger gradual gain of alignment of approximately $15\hbar$ caused first by the AB neutron alignment ($9\hbar$) followed by the A_pB_p proton alignment ($6\hbar$). Band 6 is interpreted as the unfavored $i_{13/2}$ neutron signature B, and therefore the AB and BC crossings are Pauli blocked. The alignment above $\hbar\omega \approx 0.35$ MeV in this band is interpreted as the B to BAD band crossing.

It thus appears that a A_pB_p crossing with strong interaction strength occurs in all observed bands in $N \geqslant 89$ Dy

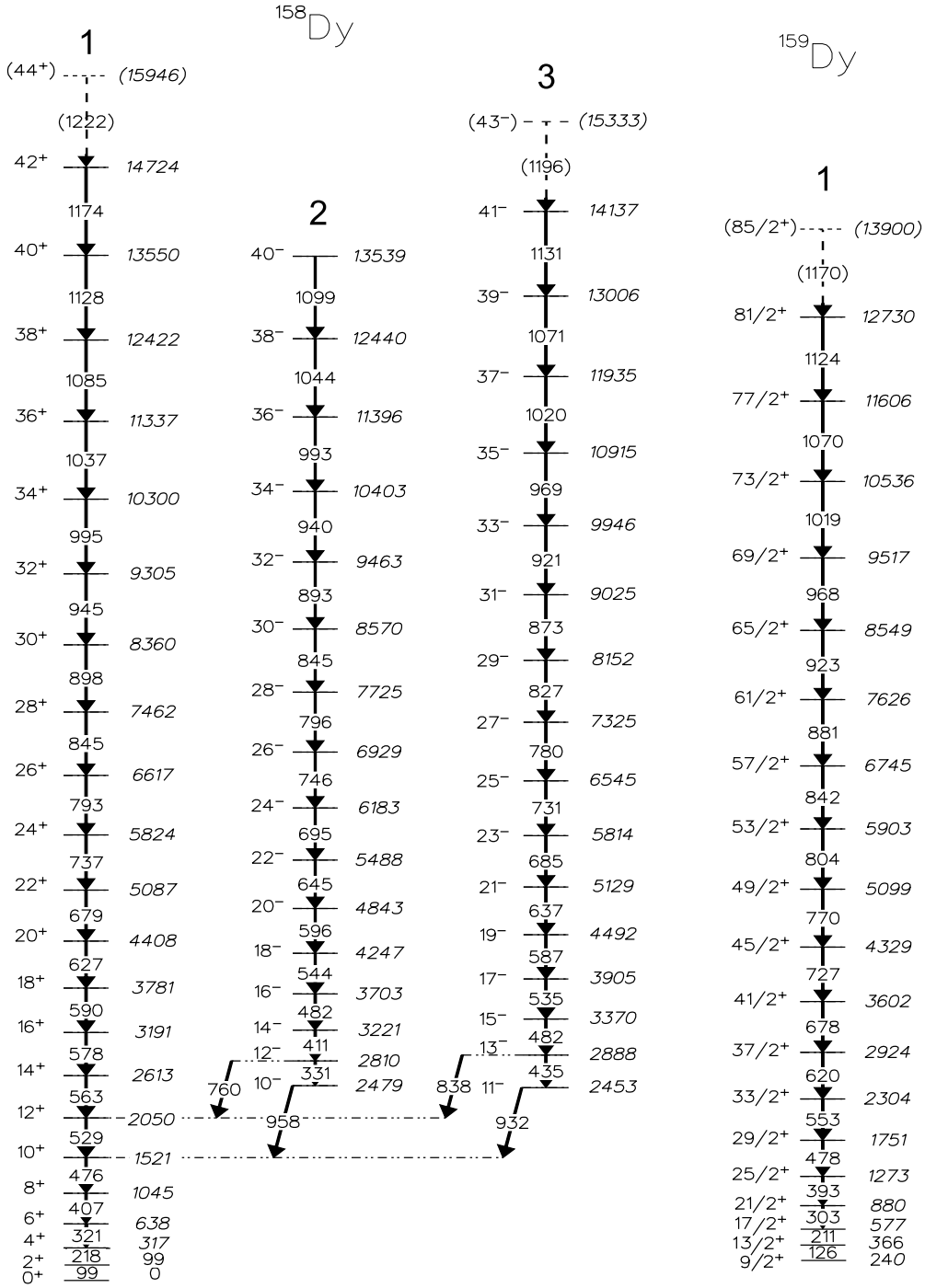

FIG. 5. The level schemes deduced for ^{158}Dy and ^{159}Dy. Energy values are in kiloelectronvolts, tentative transitions are indicated by dotted lines and tentative spin, and parity and level energies are given within parentheses.

nuclei, even though the low-spin yrast structure changes from weakly prolate deformed in the light Dy isotopes to strongly prolate deformed for the heavier ones [41]. This interpretation is in agreement with theoretical predictions regarding the oscillatory nature of the band crossing interaction strength with particle number [42–44]. However, more recent theoretical work aimed specifically at the systematics of the yrast bands in even-N Dy isotopes, such as those using the angular-momentum-projected Tamm-Dancoff model [45], still predict a more noticeable change in moment of inertia (weaker band-crossing interaction strength) for the first proton crossing (A_pB_p) than is experimentally observed.

In Fig. 10, the alignment of the yrast sequences in ^{157,158,159}Dy and some neighboring isotones observed to high spins are compared. There are many common features in these plots, including a gradual and consistent progression

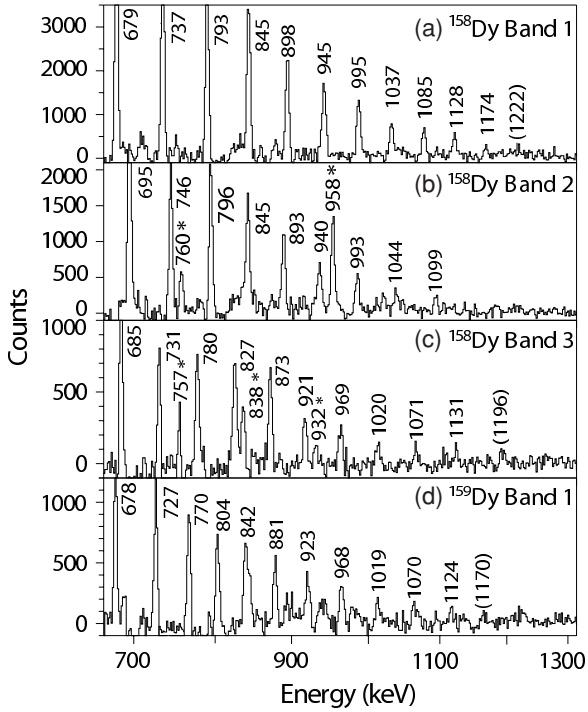

FIG. 6. Double-gated, summed coincidence spectra of (a) band 1 ($\pi, \alpha =$) (+,0), (b) band 2 (−,0), (c) band 3 (−,1) bands in ^{158}Dy, and (d) band 1 (+,+$\frac{1}{2}$) band in ^{159}Dy. The 760-, 958-, 757-, 838-, and 932-keV side-feeding transitions in ^{158}Dy are marked with asterisks.

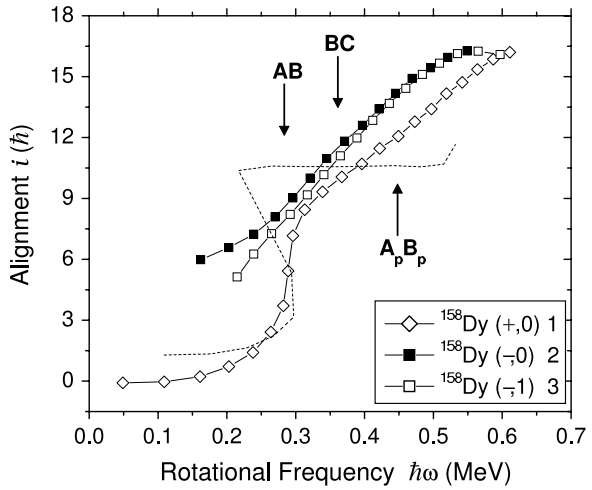

FIG. 8. Experimental alignment (i) versus rotational frequency ($\hbar\omega$) for bands in ^{158}Dy. The band crossings are labeled at the appropriate rotational frequencies [36,37]. The *AB* and *BC* labels refer to the first and second $i_{13/2}$ neutron crossings and the A_pB_p label to the first $h_{11/2}$ proton crossing. Harris parameters of $\Im_0 = 32$ MeV$^{-1}\hbar^2$ and $\Im_1 = 34$ MeV$^{-3}\hbar^4$ were used. These provide a constant alignment above $\hbar\omega = 0.2$ MeV for the three-quasiparticle configuration (B_pAB) in ^{157}Ho [38], included as a reference trajectory (dotted) for comparison.

in band-crossing interaction strengths with varying particle numbers. The linear increase in the critical band-crossing frequency $\hbar\omega_c$ with decreasing proton number for the first $i_{13/2}$ (*AB*) crossing in the $N = 92$ even-even nuclei [Fig. 10(b)] has already been documented and discussed in detail [56]. This behavior is consistent with an increase in quadrupole deformation when moving from Hf to Dy [40], which results in the neutron Fermi surface for the latter being further from the highly alignable, low-Ω components of the $i_{13/2}$ shell. A detailed comparison of the alignment frequencies in these Dy isotopes is not possible because the *BC* and A_pB_p band crossings have a strong interaction strength. However, the alignment gains and approximate critical frequencies of these band crossings form a consistent picture with those in neighboring nuclei, as shown in Fig. 10.

The alignment systematics discussed above form a coherent body of data, which are generally well described within the

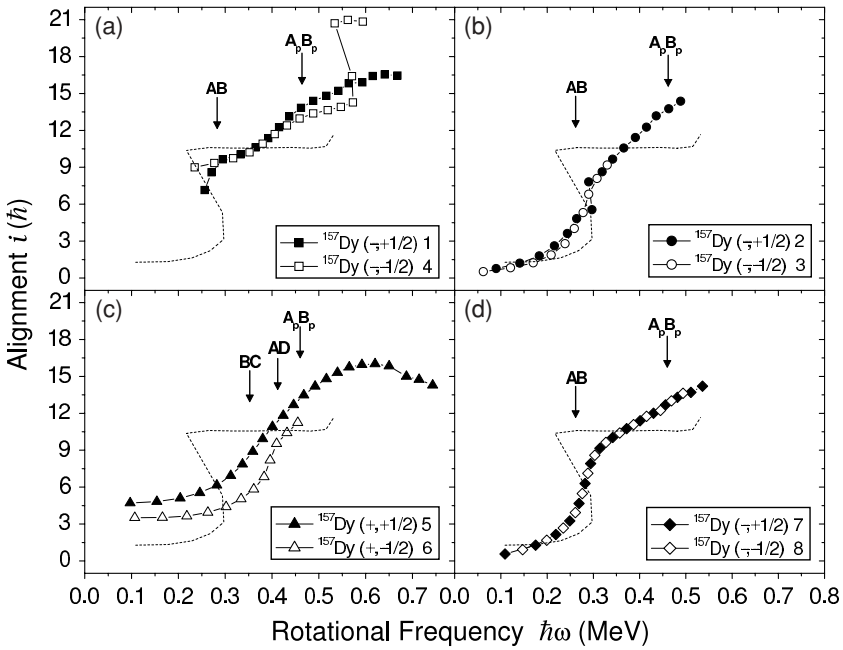

FIG. 7. Experimental alignment (i) versus rotational frequency ($\hbar\omega$) for bands in ^{157}Dy. The band crossings are labeled at the appropriate rotational frequencies [36,37]. The *AB*, *BC*, and *AD* labels refer to the first, second, and third $i_{13/2}$ neutron crossings and the A_pB_p label to the first $h_{11/2}$ proton crossing. Harris parameters of $\Im_0 = 32$ MeV$^{-1}\hbar^2$ and $\Im_1 = 34$ MeV$^{-3}\hbar^4$ were used. These provide a constant alignment above $\hbar\omega = 0.2$ MeV for the three-quasiparticle configuration (B_pAB) in ^{157}Ho [38], included as a common reference trajectory (dotted) in each of the panels.

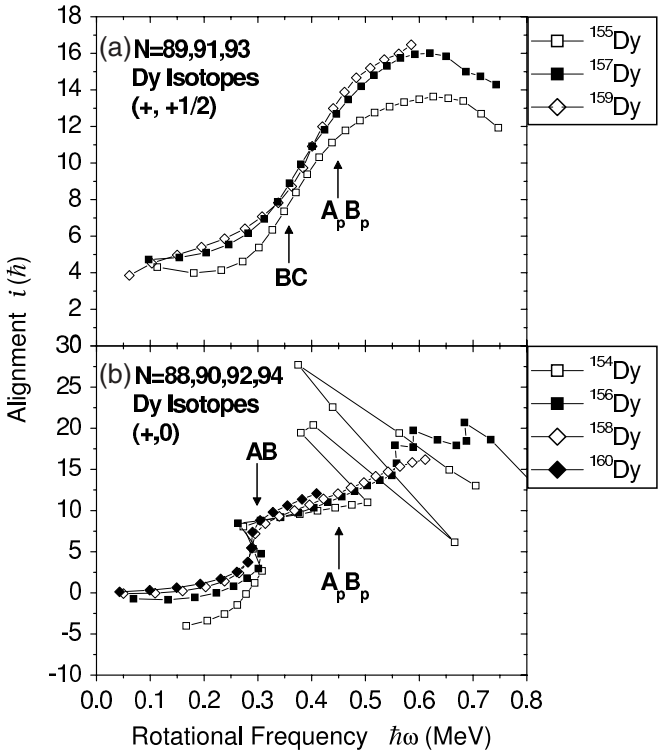

FIG. 9. Experimental alignments i versus rotational frequency $\hbar\omega$ for (a) odd-N $^{155-159}$Dy isotopes, and (b) the yrast bands of even-N,$^{154-160}$Dy. The band crossings are labeled at the appropriate rotational frequencies [36,37]. Harris parameters of $\Im_0 = 32$ MeV$^{-1}\hbar^2$ and $\Im_1 = 34$ MeV$^{-3}\hbar^4$ were used. Information for the other Dy isotopes is taken from Ref. [16](^{154}Dy), Ref. [17,18](^{155}Dy), Ref. [11] (^{156}Dy), and Ref. [40](^{160}Dy).

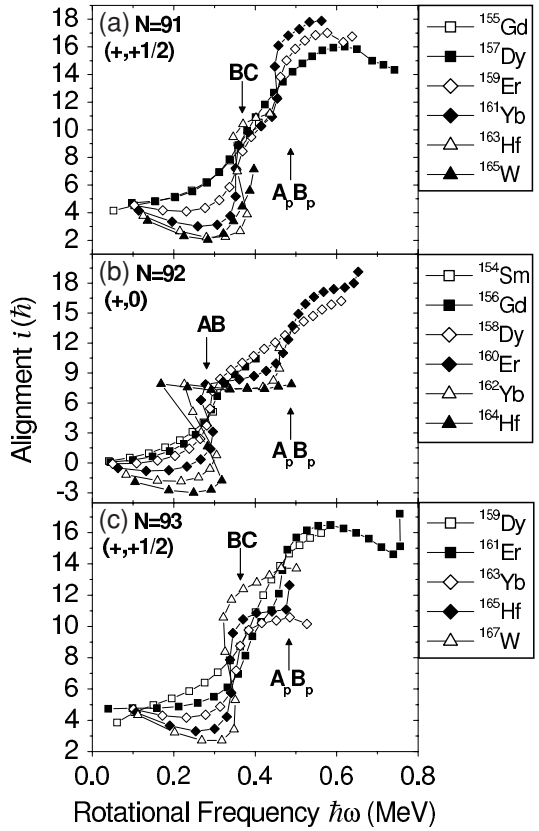

FIG. 10. Experimental alignments i versus rotational frequency $\hbar\omega$ for (a) (+,+1/2) bands in $N = 91$ isotones, (b) (+,0) bands in $N = 92$ isotones, and (c) (+,+1/2) bands in $N = 93$ isotones. The band crossings are labeled at the appropriate rotational frequencies [36,37]. Harris parameters of $\Im_0 = 32$ MeV$^{-1}\hbar^2$ and $\Im_1 = 34$ MeV$^{-3}\hbar^4$ were used. References (apart from the Dy isotopes presented in this work) are as follows: (a) for $N = 91$ isotones Ref. [46]^{155}Gd, Ref. [4]^{159}Er, Ref. [47]^{161}Yb, Ref. [48]^{163}Hf, and Ref. [49]^{165}W; (b) for $N = 92$ isotones Ref. [50]^{154}Sm, Ref. [51]^{156}Gd, Ref. [6]^{160}Er, Ref. [52]^{162}Yb, and Ref. [10,53]^{164}Hf; and (c) $N = 93$ isotones Ref. [8]^{161}Er, Ref. [54]^{163}Yb, Ref. [53]^{165}Hf, Ref. [55]^{167}W.

cranked-shell model with pairing included [36]. However, at very high rotational frequency there are known instances where the observed alignment gains in certain configurations do not fall within the standard CSM-plus-pairing framework. Such occurrences have been investigated in the $N = 91$–94 Er isotopes [5,7,8]. It was shown that a satisfactory explanation of the alignments and energy ordering of the bands at high spins can be achieved within a framework that used a specific spectrum of single-particle orbitals in which static pairing correlations are quenched.

In ^{157}Dy, one such alignment anomaly occurs in the tentative $(-,+\frac{1}{2})$ sequence, band 4, at $\hbar\omega \approx 0.55$ MeV [see Fig. 7(a)]. To investigate this as well as the general behavior at very high spin of bands in ^{157}Dy, a detailed set of configuration-dependent cranked Nilsson-Strutinsky calculations [12,57] without pairing has been carried out. The results of these calculations for ^{157}Dy are displayed in Fig. 11(b), where different configurations, labeled by their number of occupied $N = 5\,h_{11/2}$ proton and $N = 6\,i_{13/2}$ neutron orbitals (e.g., $\pi 5^6 \nu 6^2 = [6,2]$), are given. These theoretical trajectories can be compared with the experimental bands plotted in Fig. 11(a).

In the calculations, we have used the standard Nilsson model parameters [57], but with the modification that the μ value of the $N = 6$ neutron orbitals has been increased from 0.34 to 0.40. Note that the latter value is used for the $A = 150$ parameters [58]. With this modification, our parameters are essentially equivalent to the $A = 165$ parameters of Ref. [59] for the valence oscillator shells in the deformed rare-earth region. Indeed, these $A = 165$ parameters are known to give a very accurate description of the ground-state properties of the deformed nuclei in this region.

The calculations describe the yrast band as a [6,3] configuration with the signature partner much less favored in energy. The signature partner bands 7,8 and 2,3 are then described as [6,(1)4] [high-j configuration $\pi(h_{11/2})^6\nu(h_{11/2})^{-1}(i_{13/2})^4$] and [6,2], respectively. These configurations are calculated at excitation energies and signature splittings that are roughly in agreement with experiment.

The remaining bands 1 and 4 are essentially signature degenerate up to $I \approx 30$, which means that they are most likely built from signature partner configurations. The fact that they are not seen below $I = 15$ furthermore suggests that they start out as three-quasiparticle configurations. Because the neutron $\nu(i_{13/2})^3$ configuration is strongly favored over

a large spin range, it seems most natural that they are built from this neutron configuration combined with a negative-parity proton configuration, i.e., Refs. [7,3]. This also gives a natural explanation for the crossing in band 4 as a crossing with a [5,3] configuration. Note that such crossings where two $h_{11/2}$ protons are de-excited to orbitals below the $Z = 64$ subshell gap are natural explanations in an unpaired formalism [60].

There are, however, also some problems with this interpretation for bands 1 and 4. For example, the [7,3] configuration is calculated around 0.5 MeV too high in excitation energy, so that the crossing in band 1 occurs around $I = 30$ compared with the observed value $I \approx 40$. There are three [5,3] configurations at similar energies shown in Fig.11, one with the proton configuration $\pi(g_{7/2}d_{5/2})^{-4}(h_{11/2})^5(d_{3/2})^1$ (whose signature partner is predicted to be considerably higher in energy) and two signature degenerate bands with the proton configuration $\pi(g_{7/2}d_{5/2})^{-3}(h_{11/2})^5$. It is the former band, which is lowest in energy at high spins, that is our preferred interpretation for the highest spin states in band 4. However, the presence of the other bands suggests the possibility of a similar crossing in band 1 that is not observed experimentally. One explanation could be that we need to use a different spacing between the $g_{7/2}d_{5/2}$ and the $d_{3/2}$ shells, which would affect the relative energies of the [5,3] bands.

For the description of the calculated bands in ^{157}Dy, it is instructive to introduce the quantity $I_{\max}$ defined as the maximum spin value that can be built in the pure j-shell configurations. In the ground-band configuration the noncollective $I_{\max}$ state is built as $\pi[(g_{7/2}d_{5/2})^{-4}_{10}(h_{11/2})^6_{18}]_{28}\,\nu[(h_{9/2}f_{7/2})^6_{18}(i_{13/2})^3_{16.5}]_{34.5}$, where the number of particles or holes in the different groups of orbitals is given as a superscript and the corresponding maximum spin values as a subscript. It is thus easy to calculate $I_{\max} = 62.5$. If the (groups of) j shells were pure, all spin vectors would be quantized (aligned) along the same axis in this $I_{\max}$ state and the band would get a standard termination in an axially symmetric state. The notation above does not refer to the pure j shells, however, but to the orbitals dominated by these j shells. Thus, with increasing deviation from spherical shape and with increasing rotational frequencies, the orbitals will get larger admixtures from other j shells. For example, there is a small mixture of the proton $h_{9/2}$ and $f_{7/2}$ shells into the $h_{11/2}$ orbitals and a small mixture of the $h_{11/2}$ shell into the neutron $h_{9/2}$ and $f_{7/2}$ orbitals. It then becomes possible to build the $I_{\max}$ state even though the angular momenta are not fully aligned, i.e., for a state that is not axially symmetric at $\gamma = 60^\circ$ but instead triaxial, corresponding to small collectivity. There will then be a competition between the non-collective state and a slightly collective state and depending on how the particles are distributed over j shells, one or the other will be lower in energy. Note also that even though the deformation might be away from the $\gamma = 60^\circ$ axis, there will be a large overlap with the fully aligned state in terms of how the angular momentum is built. Conversely, the shape at $I = I_{\max}$ might have a strong influence on the $B(E2)$ values for the states with I approaching $I_{\max}$. In the present calculations for the yrast band configuration ([6,3]), the energy minimum is found for $\gamma \approx 35^\circ$. However, the lowest energy for $\gamma = 60^\circ$, i.e., the lowest energy for a fully aligned state, is less than 0.1 MeV higher in energy, so from the calculations, we cannot decide if this configuration terminates in a non-collective state or not. In Fig. 11, the $I_{\max}$ are shown by large open circles or large open squares, depending on if the lowest energy minimum for this spin value is calculated at $\gamma = 60^\circ$ or at a triaxial shape.

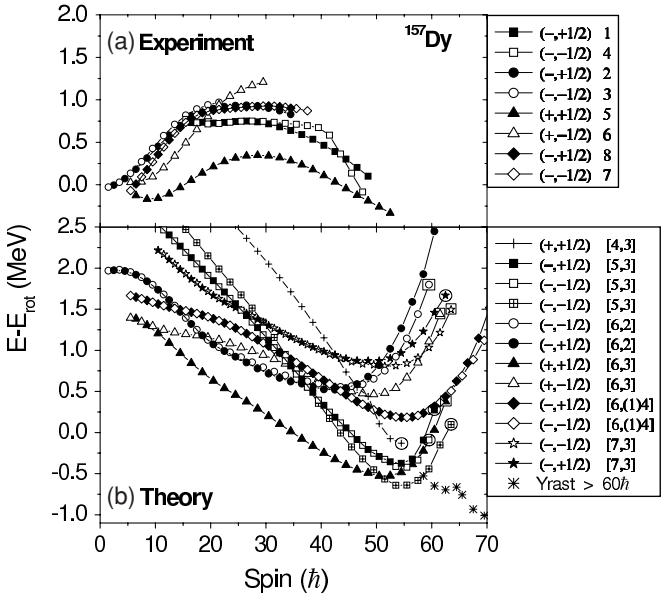

FIG. 11. The observed bands of ^{157}Dy (upper panel) and the calculated configurations drawn relative to a rigid rotor reference, $E_{\rm rot} = A \times I(I+1)$. The experimental bands are labeled by their parity, signature, and band number. The calculated configurations are labeled by their parity, signature, and the number of occupied $N = 5$, $h_{11/2}$ proton and $N = 6$, $i_{13/2}$ neutron orbitals, e.g., $\pi 5^6 \nu 6^2 =$ [6,2] (with the number of $h_{11/2}$ neutron holes in parentheses if applicable). Closed symbols are used for signature $\alpha = +1/2$ and open symbols for $\alpha = -1/2$. The $I_{\max}$ states (see text) are shown by large open circles or large open squares, depending on if the lowest energy minimum for this spin value is calculated at $\gamma = 60^\circ$ or at a triaxial shape. The present configurations build the yrast line up to $I \approx 60$, but for higher spin values configurations with protons in the higher shells, $h_{9/2}$ and $i_{13/2}$, come lower in energy as indicated by the asterisk symbols. (Note that the subtracted rigid rotor reference values [A(expt) = 0.0075 MeV and A(theory) = 0.007 MeV] have been chosen such that the slope of the (+,1/2) yrast trajectories at $I = 35\hbar$ are similar in theory and experiment. The large differences in curvature at low spin values can be traced to the fact that the calculations do not include pairing correlations.)

We have also included one band with fewer holes in the proton core in Fig. 11, namely [4,3], which has the same particle configuration (with the addition of two $d_{5/2}$ proton holes in the $Z = 64$ core) as the very favored terminating $I = 50.5^+$ state in the neighboring isotone ^{159}Er[4]. Bands of this kind with few $h_{11/2}$ protons are generally found to terminate in a more favored manner and this is indeed what we find, i.e., the terminating state in ^{157}Dy at $I = 54.5$ is lower in energy than the $I = 52.5, 50.5, \ldots$ states when drawn versus a standard reference (see Fig. 11). Furthermore, with the $A = 150$ parameters [58], this configuration actually becomes

yrast. The latter finding indicates the level of uncertainty of the relative energies in the present calculation because the $A = 150$ parameters have been commonly used when investigating the competition between collective and non-collective states in this mass region.

With increasing spin, as discussed above, nuclei in the transitional rare-earth region ($N \approx 90$) are known to undergo an angular momentum induced transition from prolate collective rotation to oblate non-collective behavior via the mechanism of band termination [12]. For the even-even Dy isotopes this shape change can be observed [see Fig. 9(b)] from the drastic change in alignment curvature in the yrast (+,0) bands for $N = 88$ [14–16] and $N = 90$ [11] at $\hbar\omega = 0.45$ and 0.55 MeV, respectively. No evidence for such a transition in ^{158}Dy can be seen up to $\hbar\omega = 0.6$ MeV and spin $44\hbar$. This is consistent with experimental results on the only other $N = 92$ nucleus, ^{160}Er, observed to such high spin values and rotational frequencies [4,6] [see Fig. 10(b)].

V. CONCLUSIONS

The latest generation of very high efficiency γ-ray detector arrays provides the opportunity to study nuclear structure phenomena at high spin in rare-earth nuclei populated at a very small fraction of the total reaction cross section and in nuclei that may not be easily accessible using standard (HI, xn) reactions. The significantly extended data on ^{157,158,159}Dy presented here show regular rotational structures up to spin $\approx 50\hbar$. All the observed bands undergo the first proton (A_pB_p) alignment with a strong interaction strength that consistently appears throughout the Dy isotopic chain. The alignment systematics in Dy isotopes also exhibit a strong interaction strength for the second $i_{13/2}$ (BC) band crossing. The latter successfully explains the previous claim of "poor agreement" between theory and experiment regarding the alignment gain at the BC neutron crossing in ^{159}Dy. An alignment that does not fit into the cranked shell model plus pairing framework that is so successful at lower spins is observed in one band in ^{157}Dy above $I = 35\hbar$. This anomaly is interpreted as an unpaired band crossing and this is consistent with the predictions of cranked Nilsson-Strutinsky calculations where static pairing correlations are assumed to be negligible. No evidence is observed for the onset of a prolate to oblate shape change in ^{158}Dy up to spin $44\hbar$, in contrast to lower mass even-even Dy isotopes.

ACKNOWLEDGMENTS

We are indebted to Dr. D. C. Radford for providing the Radware analysis codes. Support for this work was provided by the National Science Foundation, the State of Florida, and the U.S. Department of Energy Office of Nuclear Physics through contract No. W-31-109-ENG-38 (Argonne National Laboratory); the UK Engineering and Physical Sciences Research Council; the Danish Natural Science Foundation; the Swedish Science Research Council; the EU Access to Large Scale Facilities-Training and Mobility of Research Program Contract No. ERBFMGECT980110 for INFN-Laboratori Nazionali di Legnaro; and EU contract No. HPRI-CT-1999-0078 for Institut de Recherches Subatomiques, Strasbourg.

[1] J. Simpson, Z. Phys. A **358**, 139 (1997).
[2] I. Y. Lee, Nucl. Phys. **A520**, 641c (1990).
[3] R. V. F. Janssens and F. S. Stephens, Nucl. Phys. News **6**, 9 (1996).
[4] F. G. Kondev, M. A. Riley, T. B. Brown, R. M. Clark, M. Devlin, P. Fallon, D. J. Hartley, I. M. Hibbert, D. T. Joss, D. R. LaFosse, R. W. Laird, F. Lerma, M. Lively, P. J. Nolan, N. J. O'Brien, E. S. Paul, J. Pfohl, D. G. Sarantites, R. K. Sheline, S. L. Shepherd, J. Simpson, and R. Wadsworth, J. Phys. G: Nucl. Part. Phys. **25**, 897 (1999).
[5] M. A. Riley, J. D. Garrett, J. Simpson, and J. F. Sharpey-Schafer, Phys. Rev. Lett. **60**, 553 (1988).
[6] J. Simpson, M. A. Riley, A. N. James, A. R. Mokhtar, H. W. Cranmer-Gordon, P. D. Forsyth, A. J. Kirwan, D. Howe, J. D. Morrison, and J. F. Sharpey-Schafer, J. Phys. G **13**, L235 (1987).
[7] M. A. Riley, J. W. Roberts, J. Simpson, A. Alderson, I. Ali, M. A. Bentley, A. M. Bruce, R. Chapman, D. M. Cullen, P. Fallon, P. D. Forsyth, J. C. Lisle, J. N. Mo, and J. F. Sharpey-Schafer, J. Phys. G: Nucl. Phys. **16**, L67 (1990).
[8] J. Simpson, A. P. Bagshaw, A. Pipidis, M. A. Riley, M. A. Bentley, D. M. Cullen, P. J. Dagnall, G. B. Hagemann, S. L. King, R. W. Laird, J. C. Lisle, S. Shepherd, A. G. Smith, S. Tormanen, A. Afanasjev, and I. Ragnarsson, Phys. Rev. C **62**, 024321 (2000).
[9] M. A. Deleplanque, J. C. Bacelar, E. M. Beck, R. M. Diamond, J. E. Draper, R. J. McDonald, and F. S. Stephens, Phys. Lett. **B193**, 422 (1987).
[10] J. N. Mo, S. Sergiwa, R. Chapman, J. C. Lisle, E. Paul, J. C. Willmott, J. Hattula, M. Jaaskelainen, J. Simpson, P. M. Walker, J. D. Garrett, G. B. Hagemann, B. Herskind, M. A. Riley, and G. Sletten, Nucl. Phys. **A472**, 295 (1987).
[11] F. G. Kondev, M. A. Riley, R. V. F. Janssens, J. Simpson, A. V. Afanasjev, I. Ragnarsson, I. Ahmad, D. J. Blumenthal, T. B. Brown, M. P. Carpenter, P. Fallon, S. M. Fischer, G. Hackman, D. J. Hartley, C. A. Kalfas, T. L. Khoo, T. Lauritsen, W. C. Ma, D. Nisius, J. F. Sharpey-Schafer, and P. G. Varmette, Phys. Lett. **B437**, 35 (1998).
[12] I. Ragnarsson, Z. Xing, T. Bengtsson, and M. A. Riley, Phys. Scr. **34**, 651 (1986).
[13] A. Pakkanen, Y. H. Chung, P. J. Daly, S. R. Faber, H. Helppi, J. Wilson, P. Chowdhury, T. L. Khoo, I. Ahmad, J. Borggreen, Z. W. Grabowski, and D. C. Radford, Phys. Rev. Lett. **48**, 1530 (1982).
[14] H. W. Cranmer-Gordon, P. D. Forsyth, D. V. Elenkov, D. Howe, J. F. Sharpey-Schafer, M. A. Riley, G. Sletten, J. Simpson, I. Ragnarsson, Z. Xing, and T. Bengtsson, Nucl. Phys. **A465**, 506 (1987).
[15] W. C. Ma, M. A. Quader, H. Emling, T. L. Khoo, I. Ahmad, P. J. Daly, B. K. Dichter, M. Drigert, U. Garg, Z. M. Grabowski,

R. Holzmann, R. V. F. Janssens, M. Piiparinen, W. H. Trzaska, and T. F. Wang, Phys. Rev. Lett. **61**, 46 (1988).
[16] W. C. Ma, R. V. F. Janssens, T. L. Khoo, I. Ragnarsson, M. A. Riley, M. P. Carpenter, J. R. Terry, J. P. Zhang, I. Ahmad, P. Bhattacharyya, P. J. Daly, S. M. Fischer, J. H. Hamilton, T. Lauritsen, D. T. Nisius, A. V. Ramayya, R. K. Vadapalli, P. G. Varmette, J. W. Watson, C. T. Zhang, and S. J. Zhu, Phys. Rev. C **65**, 034312 (2003).
[17] R. Vlastou, C. T. Papadopoulos, M. Serris, C. A. Kalfas, N. Fotiades, S. Harissopulos, S. Kossionides, J. F. Sharpey-Schafer, E. S. Paul, P. D. Forsyth, P. J. Nolan, N. D. Ward, M. A. Riley, J. Simpson, J. C. Lisle, P. M. Walker, M. Guttormsen, and J. Rekstad, Nucl. Phys. **A580**, 133 (1994).
[18] T. B. Brown, Ph.D. thesis, Florida State University, 1998.
[19] J. Simpson, M. A. Riley, S. J. Gale, J. F. Sharpey-Schafer, M. A. Bentley, A. M. Bruce, R. Chapman, R. M. Clark, S. Clarke, J. Copnell, D. M. Cullen, P. Fallon, A. Fitzpatrick, P. D. Forsyth, S. J. Freeman, P. M. Jones, M. J. Joyce, F. Linden, J. C. Lisle, A. O. Macchiavelli, A. G. Smith, J. F. Smith, J. Sweeney, D. M. Thompson, S. Warburton, J. N. Wilson, T. Bengtsson, and I. Ragnarsson, Phys. Lett. **B327**, 187 (1994).
[20] S. J. Gale, J. Simpson, M. A. Riley, J. F. Sharpey-Schafer, E. S. Paul, M. A. Bentley, A. M. Bruce, R. Chapman, R. M. Clark, S. Clarke, J. Copnell, D. M. Cullen, P. Fallon, A. Fitzpatrick, P. D. Forsyth, S. J. Freeman, P. M. Jones, M. J. Joyce, F. Liden, J. C. Lisle, A. O. Macchiavelli, A. G. Smith, J. F. Smith, J. Sweeney, D. M. Thompson, S. Warburton, J. N. Wilson, and I. Ragnarsson, J. Phys. G: Nucl. Part. Phys. **21**, 193 (1995).
[21] F. S. Stephens, M. A. Deleplanque, R. M. Diamond, A. O. Macchiavelli, and J. E. Draper, Phys. Rev. Lett. **54**, 2584 (1985).
[22] J. Simpson *et al*., Phys. Rev. Lett. **53**, 648 (1984).
[23] A. O. Evans, E. S. Paul, J. Simpson, M. A. Riley, D. E. Appelbe, D. B. Campbell, P. T. W. Choy, R. M. Clark, M. Cromaz, P. Fallon, A. Gorgen, D. T. Joss, I. Y. Lee, A. O. Macchiavelli, P. J. Nolan, A. Pipidis, D. Ward, I. Ragnarsson, and F. Saric, Phys. Rev. Lett. **92**, 252502 (2004).
[24] J. Eberth, Prog. Part. Nucl. Phys. **28**, 495 (1992); J. Eberth, H. G. Thomas, P. von Brentano, R. M. Lieder, H. M. Jager, H. Kammerling, M. Berst, D. Gutknecht, and R. Henck, Nucl. Instrum. Methods A **369**, 135 (1996).
[25] G. Duchene, F. A. Beck, P. J. Twin, G. de France, D. Curien, L. Hana, C. W. Beausang, M. A. Bentley, P. J. Nolan, and J. Simpson, Nucl. Instrum. Methods A **432**, 90 (1999).
[26] C. W. Beausang, S. A. Forbes, P. Fallon, P. J. Nolan, P. J. Twin, J. N. Mo, J. C. Lisle, M. A. Bentley, J. Simpson, F. A. Beck, D. Curien, G. de France, G. Duchene, and D. Popescu, Nucl. Instrum. Methods A **313**, 37 (1992).
[27] D. C. Radford, Nucl. Instrum. Methods A **361**, 297 (1995).
[28] W. Klamra, S. A. Hjorth, J. Boutet, S. Andre, and D. Barnoud, Nucl. Phys. **A199**, 81 (1973).
[29] M. A. Riley, J. Simpson, M. A. Bentley, P. Fallon, P. D. Forsyth, J. C. Lisle, J. D. Morrison, E. S. Paul, J. F. Sharpey-Schafer, and P. M. Walker, Z. Phys. A **345**, 121 (1993).
[30] T. Hayakawa, Y. Toh, M. Oshima, M. Matsuda, Y. Hatsukawa, J. Katakura, H. Iimura, T. Shizuma, S. Mitarai, M. Sugawara, H. Kusakari, and Y. H. Zhang, Eur. Phys. J. A **15**, 299 (2002).
[31] T. Hayakawa, Y. Toh, M. Oshima, M. Matsuda, Y. Hatsukawa, T. Shizuma, J. Katakura, H. Iimura, S. Mitarai, Y. H. Zhang, M. Sugawara, and H. Kusakari, Phys. Rev. C **68**, 067303 (2003).
[32] M. Sugawara, S. Mitarai, H. Kusakari, M. Oshima, T. Hayakawa, Y. Toh, Y. Hatsukawa, J. Katakura, H. Iimura, Y. H. Zhang, M. Sugie, and Y. Sato, Nucl. Phys. **A699**, 450 (2002).
[33] H. Emling, E. Grosse, D. Schwalm, R. S. Simon, H. J. Wollersheim, D. Husar, and D. Pelte, Phys. Lett. **B98**, 169 (1981).
[34] X. Liang, R. Chapman, K. M. Spohr, M. B. Smith, P. Bednarczyk, S. Naguleswaran, F. Haas, G. de Angelis, S. M. Campbell, P. J. Dagnall, M. Davison, G. Duchene, T. Kroll, S. Lunardi, and D. J. Middleton, Eur. Phys. J. A **10**, 41 (2001).
[35] A. Jungclaus, B. Binder, A. Dietrich, T. Hartlein, H. Bauer, C. Gund, D. Pansegrau, D. Schwalm, D. Bazzacco, G. de Angelis, E. Farnea, A. Gadea, S. Lunardi, D. R. Napoli, C. Rossi-Alvarez, C. Ur, and G. B. Hagemann, Prog. Part. Nucl. Phys. **46**, 213 (2001).
[36] R. Bengtsson, S. Frauendorf, and F. R. May, At. Data Nucl. Data Tables **35**, 15 (1986).
[37] L. L. Riedinger, O. Andersen, S. Frauendorf, J. D. Garrett, J. J. Gaardhoje, G. B. Hagemann, B. Herskind, Y. V. Makovetzky, J. C. Waddington, M. Guttormsen, and P. O. Tjom, Phys. Rev. Lett. **44**, 568 (1980).
[38] J. Simpson, P. D. Forsyth, D. Howe, B. M. Nyako, M. A. Riley, J. F. Sharpey-Schafer, J. Bacelar, J. D. Garrett, G. B. Hagemann, B. Herskind, A. Holm, and P. O. Tjom, Phys. Rev. Lett. **54**, 1132 (1985).
[39] M. A. Riley, J. Simpson, J. F. Sharpey-Schafer, J. R. Cresswell, H. W. Cranmer-Gordon, P. D. Forsyth, D. Howe, A. H. Nelson, P. J. Nolan, P. J. Smith, N. J. Ward, J. C. Lisle, E. Paul, and P. M. Walker, Nucl. Phys. **A486**, 456 (1988).
[40] A. Jungclaus, B. Binder, A. Dietrich, T. Hartlein, H. Bauer, Ch. Gund, D. Pansegrau, D. Schwalm, J. L. Egido, Y. Sun, D. Bazzacco, G. de Angelis, E. Farnea, A. Gadea, S. Lunardi, D. R. Napoli, C. Rossi-Alvarez, C. Ur, and G. B. Hagemann, Phys. Rev. C **66**, 014312 (2002).
[41] W. Nazarewicz, M. A. Riley, and J. D. Garrett, Nucl. Phys. **A512**, 61 (1990).
[42] R. Bengtsson, I. Hamamoto, and B. Mottelson, Phys. Lett. **B73**, 259 (1978).
[43] R. Bengtsson and S. Frauendorf, Nucl. Phys. **A327**, 139 (1979).
[44] A. Faessler and M. Ploszajczak, Phys. Rev. C **22**, 2609 (1980).
[45] Y. Sun and J. L. Egido, Nucl. Phys. **A580**, 1 (2002).
[46] T. Hayakawa, M. Oshima, Y. Hatsukawa, J. Katakura, H. Iimura, M. Matsuda, S. Mitarai, Y. R. Shimizu, S. I. Ohtsubo, T. Shizuma, M. Sugawara, and H. Kusakari, Nucl. Phys. **A657**, 3 (1999).
[47] D. B. Campbell, Ph.D. thesis, Florida State University, 2004.
[48] K. P. Blume, H. Hubel, M. Murzel, J. Recht, K. Theine, H. Kluge, A. Kuhnert, K. H. Maier, A. Maj, M. Guttormsen, and A. P. De Lima, Nucl. Phys. **A464**, 445 (1987).
[49] J. Simpson, F. Hanna, M. A. Riley, A. Alderson, M. A. Bentley, A. M. Bruce, D. M. Cullen, P. Fallon, and P. Walker, J. Phys. G **18**, 1207 (1992).
[50] Nucl. Data Sheets, **85**, 171 (1998).
[51] M. Sugawara, S. Mitarai, H. Kusakari, M. Oshima, T. Hayakawa, Y. Toh, Y. Hatsukawa, J. Katakura, H. Iimura, Y. H. Zhang, M. Sugie, and Y. Sato, Nucl. Phys. **A686**, 29 (2001).
[52] J. C. Lisle, E. Paul, J. C. Willmott, J. Hattula, M. Jaaskelainen, J. Simpson, P. M. Walker, J. D. Garrett, G. B. Hagemann,

B. Herskind, M. A. Riley, and G. Sletten, Nucl. Phys. **A472**, 295 (1987).
[53] K. P. Blume, H. Hubel, M. Murzel, J. Recht, K. Theine, H. Kluge, A. Kuhnert, K. H. Maier, A. Maj, M. Guttormsen, and A. P. De Lima, Nucl. Phys. **A464**, 445 (1987).
[54] C. Schuck, F. Hannachi, R. Chapman, J. C. Lisle, J. N. Mo, E. Paul, D. J. G. Love, P. J. Nolan, A. H. Nelson, P. M. Walker, Y. Ellis-Akovali, N. R. Johnson, N. Bendjaballah, R. M. Diamond, M. A. Deleplanque, F. S. Stephens, G. Dines, and J. Draper, Proc. of the XXIII Intern. Meet. on Nucl. Struc. Phys., Bormio, January 1985, 294 Ricerca Scientifica Ed Educazione Permanente.
[55] K. Theine, A. P. Byrne, H. Hubel, M. Murzel, R. Chapman, D. Clarke, F. Khazaie, J. C. Lisle, J. N. Mo, J. D. Garrett, H. Ryde, and R. Wyss, Nucl. Phys. **A548**, 71 (1992).
[56] J. Simpson, M. A. Riley, A. Alderson, M. A. Bentley, A. M. Bruce, D. M. Cullen, P. Fallon, F. Hanna, and L. Walker, J. Phys. G: Nucl. Part. Phys. **17**, 511 (1991).
[57] T. Bengtsson and I. Ragnarsson, Nucl. Phys. **A11**, 436 (1985).
[58] T. Bengtsson, Nucl. Phys. **A512**, 124 (1990).
[59] S. G. Nilsson, C. F. Tsang, A. Sobiczewski, Z. Szymanski, S. Wycech, C. Gustafsson, I. L. Lamm, P. Moller, and B. Nilsson, Nucl. Phys. **A131**, 1 (1969).
[60] T. Bengtsson and I. Ragnarsson, Phys. Lett. **B163**, 31 (1985).